

First observation of band structure in ^{76}As : Possible chirality and octupole correlations

W. Z. Xu (许文政),^{1,2} D. P. Sun (孙大鹏),^{1,2,*} S. Y. Wang (王守宇),^{1,2,†} R. A. Bark,³ H. Hua (华辉),⁴ J. Meng (孟杰),^{4,5,6} S. Q. Zhang (张双全),⁴ P. Jones,³ S. M. Wyngaardt,⁶ C. Liu (刘晨),^{1,2} S. Wang (王硕),^{1,2} G. Y. Li (李广有),^{1,2} L. Mu (穆琳),^{1,2} H. F. Bai (白洪斐),^{1,2} X. Xiao (肖骁),^{1,2} Z. Q. Li (李志泉),^{1,2} N. B. Zhang (张乃波),^{1,2} H. Jia (贾慧),^{1,2} R. J. Guo (郭睿巨),^{1,2} X. C. Han (韩星池),^{1,2} B. Qi (齐斌),^{1,2} C. Y. Niu (牛晨阳),⁴ C. G. Wang (王春光),⁴ E. A. Lawrie,^{3,7} J. J. Lawrie,^{3,7} J. F. Sharpey-Schafer,^{3,7} M. Wiedeking,^{3,8} S. N. T. Majola,^{3,9} T. D. Bucher,^{3,6} T. Dinoko,¹⁰ B. Maqabuka,^{3,7} L. Makhathini,^{3,6} L. Mdletshe,^{3,11} N. A. Khumalo,^{3,7} O. Shirinda,^{3,12} and K. Sowazi³

¹Shandong Provincial Key Laboratory of Optical Astronomy and Solar-Terrestrial Environment, Institute of Space Sciences, Shandong University, Weihai 264209, People's Republic of China

²WeiHai Research Institute of Industrial Technology of Shandong University, Shandong University, Weihai 264209, People's Republic of China

³iThemba LABS, 7129 Somerset West, South Africa

⁴School of Physics and State Key Laboratory of Nuclear Physics and Technology, Peking University, Beijing 100871, People's Republic of China

⁵School of Physics and Nuclear Energy Engineering, Beihang University, Beijing 100191, People's Republic of China

⁶Department of Physics, University of Stellenbosch, Matieland 7602, South Africa

⁷Physics Department, University of the Western Cape, Private Bag X17, Bellville 7535, South Africa

⁸School of Physics, University of the Witwatersrand, Johannesburg 2050, South Africa

⁹Department of Physics, University of Cape Town, Rondebosch 7700, South Africa

¹⁰Department of Physical and Electrical Metrology, NMISA, Private Bag X34, Lynnwood Ridge, Pretoria 0040, South Africa

¹¹University of Zululand, Private Bag X1001, KwaDlangezwa 3886, South Africa

¹²Department of Physical and Earth Sciences, Sol Plaatje University, Private Bag X5008, Kimberley 8301, South Africa



(Received 29 July 2023; accepted 23 February 2024; published 1 April 2024)

High-spin states in ^{76}As have been observed for the first time by using the $^4\text{He} + ^{74}\text{Ge}$ reaction at beam energies of 58.6 and 62.6 MeV. Two positive-parity and three negative-parity bands have been found in ^{76}As . The two positive-parity bands with $\pi g_{9/2} \otimes \nu g_{9/2}$ configurations are tentatively interpreted as chiral doublet bands, which are supported by triaxial particle rotor model calculations. The electric dipole transitions linking the yrast positive- and negative-parity bands are also observed in this work, implying the possible presence of octupole correlations in ^{76}As .

DOI: [10.1103/PhysRevC.109.044303](https://doi.org/10.1103/PhysRevC.109.044303)

I. INTRODUCTION

The investigation of high-spin states in atomic nuclei is a critical aspect of nuclear physics that is indispensable for comprehending nuclear structure and its fundamental characteristics. For the past few decades, the high-spin states of atomic nuclei have been extensively studied thanks to the advancements in accelerators and large-scale detector arrays. These research endeavors have led to the discovery of several intriguing nuclear structural phenomena, such as backbending [1] superdeformed bands [2], octupole bands [3], and chiral doublet bands [4]. It should be noted that there is still a limited amount of data available on high-spin states in nuclei located near the stability line and in neutron-rich regions. This is primarily due to the limited accessibility of these nuclei through fusion-evaporation reactions using stable beam/target combinations.

Chiral symmetry breaking in atomic nuclei has attracted considerable attention since it was first predicted by Frauendorf and Meng [4]. They pointed out that, in the intrinsic frame of the rotating triaxial nucleus, the angular momenta of high- j particles and high- j holes align along the short and long axes, respectively, and the angular momentum of the core aligns with the intermediate axis. The three mutually perpendicular angular momenta construct the chiral geometry and result in the formation of two chiral systems, namely, left- and right-handed orientations. The restoration of spontaneous chiral symmetry breaking in the laboratory frame may give rise to pairs of nearly degenerate $\Delta I = 1$ bands with the same parity, which are called chiral doublet bands [4]. Up to now, lots of candidate chiral doublet bands have been found in the $A \approx 80, 100, 130,$ and 190 mass regions [5–12]. In the $A \approx 80$ mass region, chirality has been systematically studied, where chiral doublet bands can be formed with $\pi g_{9/2} \otimes \nu g_{9/2}$ configurations [13–19]. In Br isotopes, the coexistence of chiral doublet bands and octupole correlations has been observed, enabling the systematic study of the evolution of chiral geometry with neutron number in the presence of octupole

*sundapeng@sdu.edu.cn

†sywang@sdu.edu.cn

correlations [13–16]. In ^{84}Rb , a pair of positive-parity doublet bands was suggested as chiral vibration. The lack of static chirality in ^{84}Rb may be attributed to the deviation of the valence proton from ideal particlelike behavior [17]. Recently, chirality and octupole correlations also have been reported in ^{74}As [18]. It is worth mentioning that As isotopes are expected to possess a more stable chiral geometry compared to the Br and Rb isotopes because they have fewer valence protons, making them closer to the ideal particlelike configuration. Exploring the evolution of chiral geometry in the presence of octupole correlations in As isotopes is particularly important for obtaining systematic insights into chirality and octupole correlations in the $A \approx 80$ mass region. However, information on high-spin states for As isotopes on the neutron-rich side near the line of stability is scarce; in particular, high-spin states of ^{76}As have not been observed. In order to supplement the nuclear structure information of As isotopes and carry out a systematic study, the current work focuses on investigating the high-spin states of ^{76}As .

II. EXPERIMENTAL DETAILS

The fusion-evaporation reaction involving the bombardment of ^4He or weakly bound ^7Li projectiles on a relatively neutron-rich target is an effective method for populating high-spin states of nuclei in the neutron-rich side near the stability line [20,21]. In the present work, high-spin states of ^{76}As were populated via the $^4\text{He} + ^{74}\text{Ge}$ reaction at beam energies of 58.6 and 62.6 MeV. The beam was delivered by the Separated Sector Cyclotron of iThemba LABS, South Africa. The target consisted of 2.85 mg/cm^2 ^{74}Ge with a 10.8 mg/cm^2 carbon backing. The emitted γ rays were detected by the AFRODITE array [22] which consists of eight Compton-suppressed clover detectors and two low-energy photon spectrometer detectors. A total of 1.9×10^9 twofold and higher prompt γ -ray coincidence events were collected and sorted into several symmetric and asymmetric matrices. The two-dimensional (E_γ - E_γ) and three-dimensional (E_γ - E_γ - E_γ) symmetric matrices were used for γ - γ coincidence analyses, and the two-dimensional (E_γ - E_γ) asymmetric matrices were used to perform the angular distributions from oriented states (ADO) [23] and polarization asymmetry (A_p) measurements [24]. In this experiment, typical ADO ratios ≈ 1.2 are expected for stretched quadrupole transitions or $\Delta I = 0$ pure dipole transitions and ≈ 0.8 for the stretched pure dipole transitions. The positive and negative A_p values correspond to the stretched electric and the stretched magnetic transitions, respectively [24–26]. More details of the experimental setup and procedure can be found in Refs. [18,27]. The obtained γ -ray energies, excitation energies for the initial states, relative intensities, spin-parity assignments for the initial and final states, and ADO ratios of the transitions in ^{76}As are listed in Table I.

III. EXPERIMENTAL RESULTS

Prior to this work, the excited states in ^{76}As were studied by using $^{76}\text{Ge}(p, n)$ [28], $^{75}\text{As}(d, p)$ [29], $^{75}\text{As}(n, \gamma)$ [30], $^{76}\text{Se}(d, ^2\text{He})$ [31], $^{76}\text{Ge}(^3\text{He}, t)$ [32,33], and $^{76}\text{Se}(\mu^-, \nu)$ [34] reactions, and the 2^- ground state was assigned the

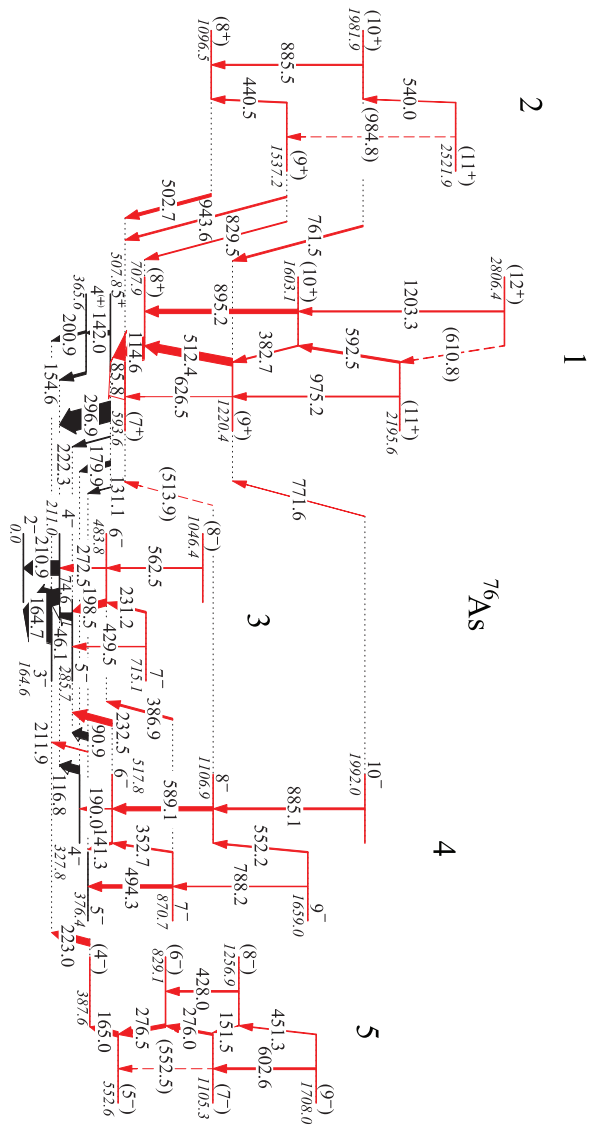


FIG. 1. Partial level scheme of ^{76}As . The energies of the γ transitions and levels are given in keV. The thicknesses of the arrows correspond to the γ -ray intensities. New transitions and levels are shown in red.

$\pi f_{5/2} \otimes \nu g_{9/2}$ configuration [28]. However, no high-spin states of this nucleus have been reported up to now. In the present work, we first reported the high-spin states in ^{76}As and identified a pair of positive-parity bands (bands 1 and 2) and three negative-parity bands (bands 3, 4, and 5), as shown in Fig. 1. The new transitions were identified on the basis of the coincidence relationships with known transitions, such as 164.7, 296.9 keV, etc. The positive-parity bands 1 and 2 decay to the 5^+ state; Figs. 2(a) and 2(b) show the typical gated spectra for the corresponding transitions of bands 1 and 2. For the negative-parity bands, band 4 decays to band 3, which is built on the 2^- ground state via several linking transitions; typical gated spectra for the corresponding transitions are shown in Figs. 2(a) and 2(c). Figures 2(a) and 2(d) exhibit the typical gated spectra showing the placement of band 5.

TABLE I. γ -ray energies, excitation energies for the initial states, relative intensities, spin-parity assignments for the initial and final states, and ADO ratios of the transitions in ^{76}As . The γ -ray energies are accurate to ± 0.5 keV.

E_γ (keV)	E_i (keV)	I_γ	$I_i^\pi \rightarrow I_f^\pi$	ADO ratio
46.1	211.0	30.5(4.4)	$4^- \rightarrow 3^-$	
74.6	285.7	40.5(3.0)	$5^- \rightarrow 4^-$	0.91(0.07)
85.8	593.6	39.5(3.4)	$(7^+) \rightarrow 5^+$	1.12(0.12)
90.9	376.4	13.1(1.4)	$5^- \rightarrow 5^-$	1.15(0.12)
114.6	707.9	41.0(3.1)	$(8^+) \rightarrow (7^+)$	0.85(0.06)
116.8	327.8	14.4(1.0)	$4^- \rightarrow 4^-$	1.24(0.09)
131.1	507.8	1.1(0.2)	$5^+ \rightarrow 5^-$	
141.3	517.8	4.0(0.5)	$6^- \rightarrow 5^-$	0.64(0.06)
142.0	507.8	15.1(1.1)	$5^+ \rightarrow 4^{(+)}$	0.72(0.05)
151.5	1256.9	< 0.5	$(8^-) \rightarrow (7^-)$	
154.6	365.6	8.8(0.8)	$4^{(+)} \rightarrow 4^-$	1.25(0.09)
164.7	164.6	100.0	$3^- \rightarrow 2^-$	0.81(0.06)
165.0	552.6	9.0(0.8)	$(5^-) \rightarrow (4^-)$	0.84(0.06)
179.9	507.8	9.6(0.7)	$5^+ \rightarrow 4^-$	0.84(0.06)
190.0	517.8	< 0.5	$6^- \rightarrow 4^-$	
198.5	483.8	12.9(1.0)	$6^- \rightarrow 5^-$	0.91(0.07)
200.9	365.6	6.5(0.7)	$4^{(+)} \rightarrow 3^-$	0.76(0.08)
210.9	211.0	27.1(2.0)	$4^- \rightarrow 2^-$	1.25(0.09)
211.9	376.4	< 0.5	$5^- \rightarrow 3^-$	
222.3	507.8	1.6(0.2)	$5^+ \rightarrow 5^-$	1.15(0.11)
223.0	387.6	12.1(1.3)	$(4^-) \rightarrow 3^-$	0.68(0.05)
231.2	715.1	2.6(0.3)	$7^- \rightarrow 6^-$	0.67(0.08)
232.5	517.8	12.5(1.3)	$6^- \rightarrow 5^-$	0.87(0.08)
272.5	483.8	1.3(0.2)	$6^- \rightarrow 4^-$	
276.0	1105.3	4.2(1.0)	$(7^-) \rightarrow (6^-)$	
276.5	829.1	7.2(1.0)	$(6^-) \rightarrow (5^-)$	0.71(0.06)
296.9	507.8	38.1(2.8)	$5^+ \rightarrow 4^-$	0.81(0.06)
352.7	870.7	4.0(0.5)	$7^- \rightarrow 6^-$	0.74(0.06)
382.7	1603.1	2.7(0.3)	$(10^+) \rightarrow (9^+)$	0.79(0.09)
386.9	870.7	3.7(0.4)	$7^- \rightarrow 6^-$	0.91(0.10)
428.0	1256.9	3.0(0.3)	$(8^-) \rightarrow (6^-)$	1.35(0.17)
429.5	715.1	1.0(0.2)	$7^- \rightarrow 5^-$	
440.5	1537.2	1.3(0.3)	$(9^+) \rightarrow (8^+)$	
451.3	1708.0	1.3(0.2)	$(9^-) \rightarrow (8^-)$	
494.3	870.7	6.6(0.8)	$7^- \rightarrow 5^-$	1.17(0.15)
502.7	1096.5	5.7(0.5)	$(8^+) \rightarrow (7^+)$	0.93(0.10)
512.4	1220.4	15.7(1.3)	$(9^+) \rightarrow (8^+)$	0.88(0.07)
540.0	2521.9	0.6(0.2)	$(11^+) \rightarrow (10^+)$	
552.2	1659.0	2.4(0.4)	$9^- \rightarrow 8^-$	0.43(0.10)
562.5	1046.4	1.0(0.1)	$(8^-) \rightarrow 6^-$	
589.1	1106.9	6.5(0.7)	$8^- \rightarrow 6^-$	1.29(0.10)
592.5	2195.6	4.4(0.4)	$(11^+) \rightarrow (10^+)$	0.83(0.07)
602.6	1708.0	3.6(0.4)	$(9^-) \rightarrow (7^-)$	1.15(0.10)
626.5	1220.4	< 0.5	$(9^+) \rightarrow (7^+)$	
761.5	1981.9	3.2(0.3)	$(10^+) \rightarrow (9^+)$	0.82(0.07)
771.6	1992.0	0.5(0.2)	$10^- \rightarrow (9^+)$	
788.2	1659.0	2.5(0.3)	$9^- \rightarrow 7^-$	1.15(0.23)
829.5	1537.2	1.7(0.2)	$(9^+) \rightarrow (8^+)$	0.70(0.21)
885.1	1992.0	3.5(0.4)	$10^- \rightarrow 8^-$	1.16(0.18)
885.5	1981.9	2.2(0.3)	$(10^+) \rightarrow (8^+)$	1.24(0.30)
895.2	1603.1	8.5(0.7)	$(10^+) \rightarrow (8^+)$	1.18(0.09)
943.6	1537.2	2.9(0.3)	$(9^+) \rightarrow (7^+)$	1.27(0.24)
975.2	2195.6	1.7(0.3)	$(11^+) \rightarrow (9^+)$	
1203.3	2806.4	2.2(0.3)	$(12^+) \rightarrow (10^+)$	1.12(0.20)

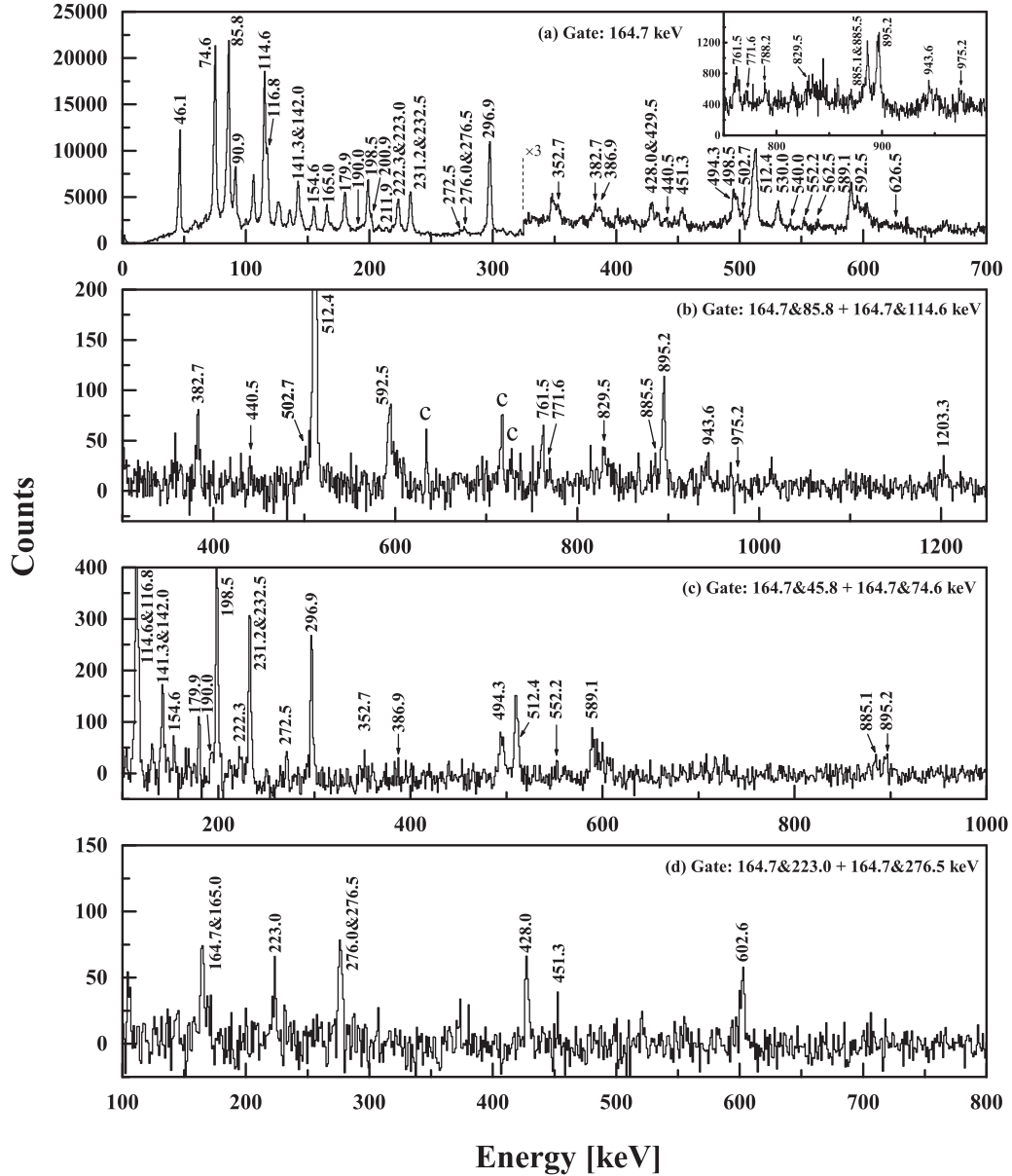


FIG. 2. (a) Typical γ - γ coincidence spectrum gated on the 164.7-keV transition showing all new transitions, and γ - γ - γ coincidence spectra (b) gated on 164.7 and 85.8 keV + 164.7 and 114.6 keV showing the placement of bands 1 and 2, (c) gated on 164.7 and 45.8 keV + 164.7 and 74.6 keV showing the placement of bands 3 and 4, and (d) gated on 164.7 and 223.0 keV + 164.7 and 276.5 keV showing the placement of band 5. Peaks labeled with a “c” are contaminant transitions.

The previously known spin-parity of the 2^- ground state has been adopted in the present work and serves as a basis for the spin-parity assignments of the other states using the measured ADO ratios and A_p values. Reference [30] suggested 3^- and 4^- assignments for the 164.6- and 211.0-keV states, respectively, and tentatively suggested (3^-) , 4^- , or 5^- for 285.7-keV state. In Ref. [29], a tentative 5^- was assigned for the 285.7-keV state. Combined with the ADO ratio analysis in the present work, we suggested 3^- , 4^- and 5^- for 164.6-, 211.0- and 285.7-keV states, respectively. In Ref. [30], (3^-) or $(4-5)^-$ were assigned to the state at 507.8 keV due to the 179.9-keV transition having an $E2$ character. However, from the present ADO ratio analysis, the 179.9-keV transition should have a $\Delta I = 1$ dipole type. In addition, an $E1$ character

to the 296.9-keV transition (decays to 4^-) is assigned based on the positive A_p value of 0.11(0.04) and the ADO ratio of 0.81(0.06), thus determining 5^+ for the state at 507.8 keV. It should be mentioned that only one A_p value for the 296.9-keV transition in ^{76}As could be accurately extracted due to the limited statistics. The spin-parity assignments for the higher spin levels of bands 1–5 were based on ADO ratios and empirical rotational band structures.

IV. DISCUSSION

As shown in Fig. 1, the present work found two positive-parity bands 1 and 2 in ^{76}As . The aligned angular momenta of these positive-parity bands are approximately $5\hbar$ greater than

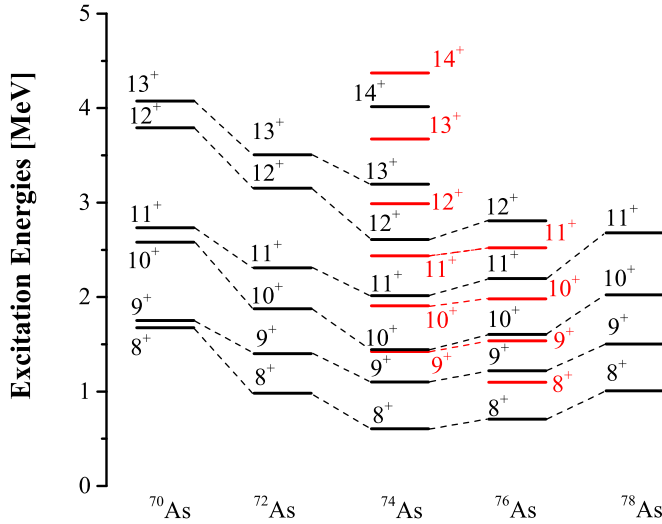


FIG. 3. The systematics of the excitation energies for the positive yrast (black) and side (red) bands above 7^+ in $^{70-78}\text{As}$ [18,35–37]. The states of ^{76}As were deduced from the present work.

that of the even-even ^{74}Ge ground-state band; such a large alignment can be obtained only for the $\pi g_{9/2} \otimes \nu g_{9/2}$ configuration in this mass region. In As isotopes, the positive-parity yrast bands in ^{70}As [35], ^{72}As [36], ^{74}As [18], and ^{78}As [37] were assigned the $\pi g_{9/2} \otimes \nu g_{9/2}$ configuration. In addition, a positive-parity side band with the $\pi g_{9/2} \otimes \nu g_{9/2}$ configuration was also found in ^{74}As [18]. The yrast and side bands in ^{74}As were interpreted as chiral doublet bands [18]. Figure 3 presents the systematic comparison of the excitation energies of the positive-parity yrast bands in $^{70-78}\text{As}$ [18,35–37] and the side bands in $^{74,76}\text{As}$ [18]. One can see in Fig. 3 that the excitation energies of states with the same spins show a smooth decrease from ^{70}As to ^{74}As and an increase from ^{74}As to ^{78}As , which follows the systematic trend. It implies that bands 1 and 2 in ^{76}As should have the same $\pi g_{9/2} \otimes \nu g_{9/2}$ configuration as the positive-parity bands in other As isotopes. Band 2 decays to band 1 via several $M1/E2$ and $E2$ linking transitions, which also suggests that band 2 has the same configuration as band 1, as discussed in Ref. [38]. Similar positive-parity doublet bands with the $\pi g_{9/2} \otimes \nu g_{9/2}$ configuration were also observed in odd-odd ^{74}As [18], $^{76-82}\text{Br}$ [13–16], and ^{84}Rb [17] and interpreted as chiral doublet bands. The systematic observation of the nearly degenerate doublet bands with the $\pi g_{9/2} \otimes \nu g_{9/2}$ configuration in the $A \approx 80$ mass region implies the same physical origin for these bands. Therefore, bands 1 and 2 in ^{76}As are likely to be a pair of chiral doublet bands.

To investigate the characteristics of bands 1 and 2 in ^{76}As , the excitation energies $E(I)$, the energy staggering parameters $S(I)$, and the reduced transition probability ratios $B(M1)/B(E2)$ for bands 1 and 2 are shown in Figs. 4(a), 4(b), and 4(c), respectively. The doublet bands exhibit nearly degenerate states and smooth variation of $S(I)$ as a function of spin, as shown in Figs. 4(a) and 4(b), respectively. In addition, it can be seen from Fig. 4(c) that the $B(M1)/B(E2)$ values of bands 1 and 2 are close and show odd-even staggering with

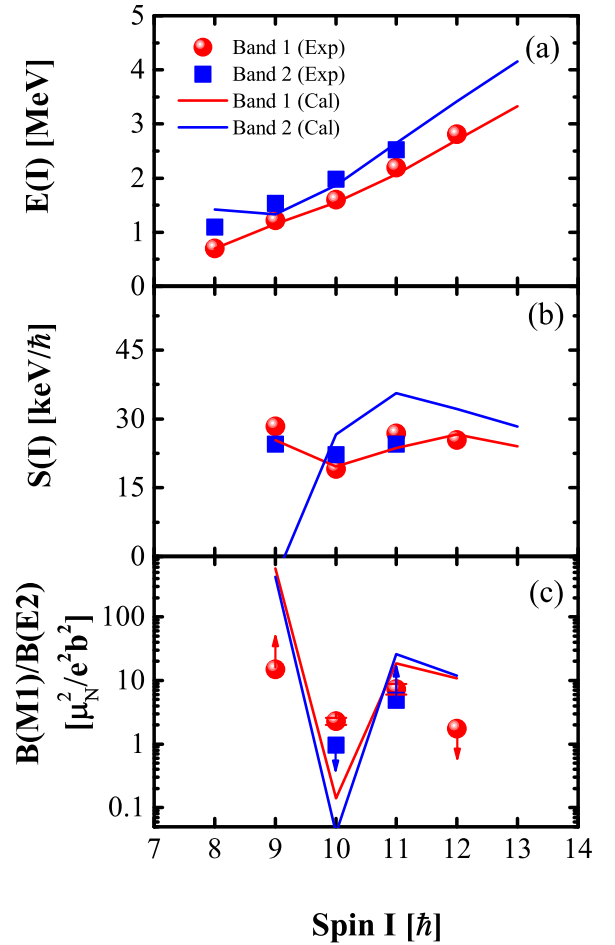


FIG. 4. The experimental excitation energies $E(I)$, energy staggering parameters $S(I) = [E(I) - E(I - 1)]/2I$, and reduced transition probability ratios $B(M1)/B(E2)$ as functions of spin for bands 1 and 2 in ^{76}As in comparison with the TPRM calculations.

the same phase. These experimental properties are consistent with the fingerprints of the chiral doublet bands [7,39–41].

Triaxial particle rotor model (TPRM) calculations [42–45] were performed to further understand the chirality in ^{76}As . The deformation parameters $(\beta_2, \gamma) = (0.37, 27.0)$ for the $\pi g_{9/2} \otimes \nu g_{9/2}$ configuration of ^{76}As were calculated using the relativistic mean-field calculations [46]. The deformation parameter $\beta_2 = 0.37$ was used as input to the present TPRM calculations. To reproduce the experimental data for bands 1 and 2, a slightly larger triaxial deformation of $\gamma = 30^\circ$ was used in TPRM calculations. The calculated $E(I)$, $S(I)$, and $B(M1)/B(E2)$ values for bands 1 and 2 are shown in Fig. 4, in comparison with the present experimental data. One can see that the small energy differences between bands 1 and 2 are well reproduced, as well as the $S(I)$ values and the trend of the $B(M1)/B(E2)$ ratios. To exhibit the chiral geometry in ^{76}As , the root-mean-square values of the angular momentum components for the core, the valence proton, and the valence neutron of the doublet bands are calculated following Refs. [13,15,16,18]. The present calculated results are shown in Fig. 5, in which $k = i, l$, and s represent the intermediate, short, and long axes, respectively. In Fig. 5, the angular

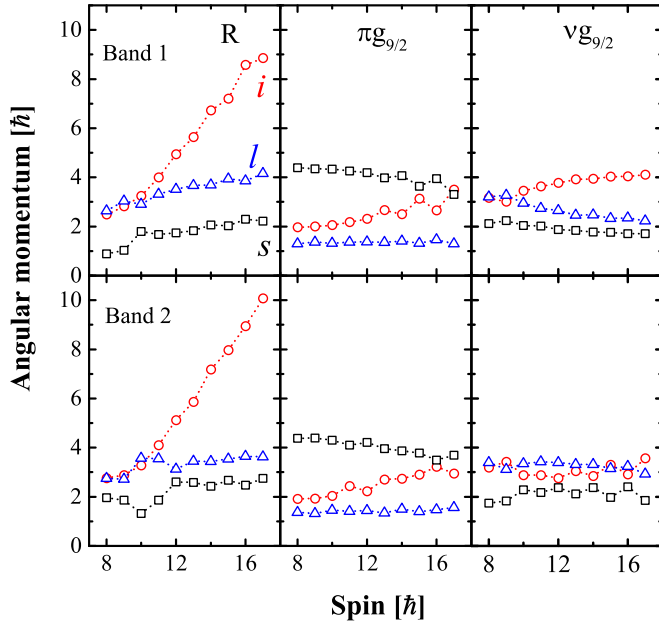


FIG. 5. The root-mean-square components along the intermediate (*i*, circles), short (*s*, squares), and long (*l*, triangles) axes of the core, valence neutron, and valence proton angular momenta calculated as functions of spin by means of the particle rotor model for the doublet bands in ^{76}As . “R” represents the core, “ $\pi g_{9/2}$ ” represents the unpaired proton in $g_{9/2}$ orbital, and “ $\nu g_{9/2}$ ” represents the unpaired neutron in $g_{9/2}$ orbital.

momenta of the core and the valence proton in ^{76}As are mainly aligned along the intermediate and the short axes, respectively. Meanwhile, the angular momentum of the valence neutron in ^{76}As shows a mixture between the intermediate and the long axes. The above results show that the total angular momentum is aplanar, which allows bands 1 and 2 to be interpreted as chiral doublet bands.

Besides positive-parity doublet bands, the negative-parity bands 3 and 4 also form a pair of doublet bands with linking transitions, suggesting similar intrinsic configurations for both bands. Band 3 is built on the 2^- ground state with the $\pi f_{5/2} \otimes \nu g_{9/2}$ configuration. It should be noted that the $f_{5/2}$ and $p_{3/2}$ orbitals are pseudospin partner orbitals, and pseudospin-chiral triplet bands involving the $\pi(p_{3/2}, f_{5/2})$ pseudospin doublet have been reported in ^{81}Kr [19]. Considering the strong mixing of these two pseudospin partner orbitals, the $\pi(p_{3/2}, f_{5/2}) \otimes \nu g_{9/2}$ configuration was tentatively assigned to bands 3 and 4. For band 5, the $\pi g_{9/2} \otimes \nu(p_{3/2}, f_{5/2})$ configuration is a candidate according to the Nilsson diagram.

In the $A \approx 80$ mass region, the proton numbers are close to 34, which may lead to the presence of octupole correlations [47]. Octupole correlations were observed in $^{72,74,78,79}\text{Se}$ [48–51], $^{74,78}\text{As}$ [18,37], and $^{76,78}\text{Br}$ [14,16] via in-beam γ -ray spectroscopy using a fusion-evaporation reaction in this mass region [52]. In addition, octupole collectivity in ^{72}Se and $^{74,76}\text{Kr}$ was studied via inelastic proton scattering in inverse kinematics recently [53]. In the present work, the observation of the linking $E1$ transitions between positive-parity band 1 and negative-parity band 4 may indicate the

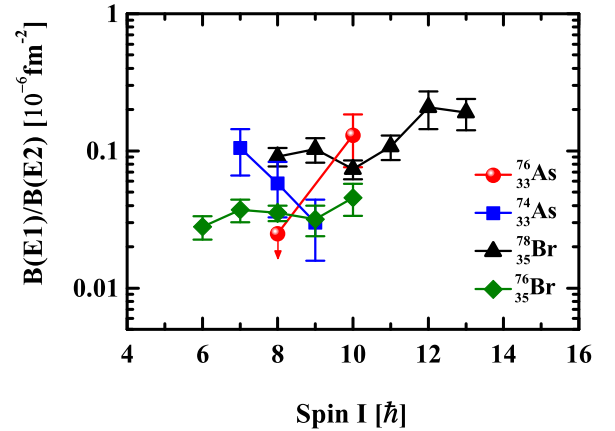


FIG. 6. The experimental $B(E1)/B(E2)$ ratios between the positive- and negative-parity bands as a function of spin in ^{76}As , together with those in ^{74}As [18], ^{78}Br [14], and ^{76}Br [16].

presence of octupole correlations in ^{76}As . To further study the octupole correlations in ^{76}As , one value and an upper limit of $B(E1)/B(E2)$ ratios in ^{76}As were obtained and are shown in Fig. 6, in comparison with those in odd-odd ^{74}As [18], ^{76}Br [16], and ^{78}Br [14]. In Fig. 6, the $B(E1)/B(E2)$ ratios in ^{76}As are comparable with those in $^{76,78}\text{Br}$ and ^{74}As , which indicates the enhancement of $B(E1)/B(E2)$ ratios in ^{76}As supporting the possible presence of octupole correlations.

V. SUMMARY

In summary, high-spin states of ^{76}As were observed for the first time via the $^4\text{He} + ^{74}\text{Ge}$ reaction. A pair of nearly degenerate positive-parity bands 1 and 2, a pair of nearly degenerate negative-parity bands 3 and 4, and a negative-parity band 5 were observed. Based on the observed band structures, $\pi g_{9/2} \otimes \nu g_{9/2}$, $\pi(p_{3/2}, f_{5/2}) \otimes \nu g_{9/2}$, and $\pi g_{9/2} \otimes \nu(p_{3/2}, f_{5/2})$ configurations were assigned to bands 1 and 2, bands 3 and 4, and band 5, respectively. The positive-parity bands 1 and 2 are tentatively interpreted as candidate chiral doublet bands. Calculations based on TPRM have been performed to investigate bands 1 and 2, which support the chiral interpretation of the doublet bands. The presence of $E1$ transitions between the opposite-parity bands 1 and 4 indicates possible octupole correlations in ^{76}As . The present work implies that chiral doublet bands (bands 1 and 2), pseudospin doublet bands (bands 3 and 4), and octupole correlations may coexist in ^{76}As , which needs to be verified by further experiments with higher statistics and lifetime measurements.

ACKNOWLEDGMENTS

This work is partly supported by the National Natural Science Foundation of China (Grants No. 12225504, No. 12075137, No. 12075138, and No. 11905113), the Major Program of Natural Science Foundation of Shandong Province (Grant No. ZR2020ZD30), the Outstanding Youth Fund of Natural Science Foundation of Shandong Province (Grant No. ZR2020YQ07), the Young Scholars Program of Shandong University, Weihai, and the National Research

Foundation in South Africa (Grants No. 92791, No. 92792, and No. 90741). The numerical calculations in this paper have been done on the supercomputing system in Shandong

University, Weihai. The authors thank the iThemba LABS technical staff and accelerator group for their support during this experiment.

- [1] A. Johnson, H. Ryde, and J. Sztarkie, *Phys. Lett. B* **34**, 605 (1971).
- [2] Y. Schutz, J. P. Vivien, F. A. Beck, T. Byrski, C. Gehringer, J. C. Merdinger, J. Dudek, W. Nazarewicz, and Z. Szymanski, *Phys. Rev. Lett.* **48**, 1534 (1982).
- [3] R. R. Chasman, *Phys. Lett. B* **96**, 7 (1980).
- [4] S. Frauendorf and J. Meng, *Nucl. Phys. A* **617**, 131 (1997).
- [5] S. Frauendorf, *Rev. Mod. Phys.* **73**, 463 (2001).
- [6] J. Meng, B. Qi, S. Q. Zhang, and S. Y. Wang, *Mod. Phys. Lett. A* **23**, 2560 (2008).
- [7] J. Meng and S. Q. Zhang, *J. Phys. G: Nucl. Part. Phys.* **37**, 064025 (2010).
- [8] R. A. Bark, E. O. Lieder, R. M. Lieder, E. A. Lawrie, J. J. Lawrie, S. P. Bvumbi, N. Y. Kheswa, S. S. Ntshangase, T. E. Madiba, P. L. Masiteng, S. M. Mullins, S. Murray, P. Papka, O. Shirinda, Q. B. Chen, S. Q. Zhang, Z. H. Zhang, P. W. Zhao, C. Xu, J. Meng *et al.*, *Int. J. Mod. Phys. E* **23**, 1461001 (2014).
- [9] K. Starosta and T. Koike, *Phys. Scr.* **92**, 093002 (2017).
- [10] B. W. Xiong and Y. Y. Wang, *At. Data Nucl. Data Tables* **125**, 193 (2019).
- [11] S. Y. Wang, *Chin. Phys. C* **44**, 112001 (2020).
- [12] S. Y. Wang, C. Liu, B. Qi, W. Z. Xu, and H. Zhang, *Front. Phys.* **18**, 64601 (2023).
- [13] S. Y. Wang, B. Qi, L. Liu, S. Q. Zhang, H. Hua, X. Q. Li, Y. Y. Chen, L. H. Zhu, J. Meng, S. M. Wyngaardt, P. Papka, T. T. Ibrahim, R. A. Bark, P. Datta, E. A. Lawrie, J. J. Lawrie, S. N. T. Majola, P. L. Masiteng, S. M. Mullins, J. Gál *et al.*, *Phys. Lett. B* **703**, 40 (2011).
- [14] C. Liu, S. Y. Wang, R. A. Bark, S. Q. Zhang, J. Meng, B. Qi, P. Jones, S. M. Wyngaardt, J. Zhao, C. Xu, S.-G. Zhou, S. Wang, D. P. Sun, L. Liu, Z. Q. Li, N. B. Zhang, H. Jia, X. Q. Li, H. Hua, Q. B. Chen *et al.*, *Phys. Rev. Lett.* **116**, 112501 (2016).
- [15] C. Liu, S. Y. Wang, B. Qi, S. Wang, D. P. Sun, Z. Q. Li, R. A. Bark, P. Jones, J. J. Lawrie, L. Masebi, M. Wiedeking, J. Meng, S. Q. Zhang, H. Hua, X. Q. Li, C. G. Li, R. Han, S. M. Wyngaardt, B. H. Sun, L. H. Zhu *et al.*, *Phys. Rev. C* **100**, 054309 (2019).
- [16] W. Z. Xu, S. Y. Wang, C. Liu, X. G. Wu, R. J. Guo, B. Qi, J. Zhao, A. Rohilla, H. Jia, G. S. Li, Y. Zheng, C. B. Li, X. C. Han, L. Mu, X. Xiao, S. Wang, D. P. Sun, Z. Q. Li, Y. M. Zhang, C. L. Wang *et al.*, *Phys. Lett. B* **833**, 137287 (2022).
- [17] X. C. Han, S. Y. Wang, B. Qi, C. Liu, S. Wang, D. P. Sun, Z. Q. Li, H. Jia, R. J. Guo, X. Xiao, L. Mu, X. Lu, Q. Wang, W. Z. Xu, H. W. Li, X. G. Wu, Y. Zheng, C. B. Li, T. X. Li, Z. Y. Huang *et al.*, *Phys. Rev. C* **104**, 014327 (2021).
- [18] X. Xiao, S. Y. Wang, C. Liu, R. A. Bark, J. Meng, S. Q. Zhang, B. Qi, H. Hua, P. Jones, S. M. Wyngaardt, S. Wang, D. P. Sun, Z. Q. Li, N. B. Zhang, H. Jia, R. J. Guo, X. C. Han, L. Mu, X. Lu, W. Z. Xu *et al.*, *Phys. Rev. C* **106**, 064302 (2022).
- [19] L. Mu, S. Y. Wang, C. Liu, B. Qi, R. A. Bark, J. Meng, S. Q. Zhang, P. Jones, S. M. Wyngaardt, H. Jia, Q. B. Chen, Z. Q. Li, S. Wang, D. P. Sun, R. J. Guo, X. C. Han, W. Z. Xu, X. Xiao, P. Y. Zhu, H. W. Li *et al.*, *Phys. Lett. B* **827**, 137006 (2022).
- [20] J. Döring, G. D. Johns, D. J. Hartley, R. A. Kaye, K. W. Kemper, G. N. Sylvan, and S. L. Tabor, *Z. Phys. A* **354**, 345 (1996).
- [21] W. Z. Xu, S. Y. Wang, X. G. Wu, H. Jia, C. Liu, H. F. Bai, Y. J. Li, B. Qi, H. Y. Zhang, G. S. Li, Y. Zheng, C. B. Li, L. Mu, A. Rohilla, S. Wang, D. P. Sun, Z. Q. Li, N. B. Zhang, R. J. Guo, X. C. Han *et al.*, *Phys. Lett. B* **839**, 137789 (2023).
- [22] R. A. Bark, M. Lipoglavsek, S. M. Maliage, S. S. Ntshangase, and A. Shevchenko, *J. Phys. G: Nucl. Part. Phys.* **31**, S1747 (2005).
- [23] M. Piiparinen, A. Ataç, J. Blomqvist, G. B. Hagemann, B. Herskind, R. Julin, S. Juutinen, A. Lampinen, J. Nyberg, G. Sletten, P. Tikkanen, S. Törmänen, A. Virtanen, and R. Wyss, *Nucl. Phys. A* **605**, 191 (1996).
- [24] P. M. Jones, L. Wei, F. A. Beck, P. A. Butler, T. Byrski, G. Duchene, G. de France, F. Hannachi, G. D. Jones, and B. Kharraja, *Nucl. Instrum. Methods Phys. Res. Sect. A* **362**, 556 (1995).
- [25] T. E. Madiba, Directional correlation from oriented states and linear polarization measurements of gamma rays from ^{190}Tl , M.Sc. thesis, University of the Western Cape, 2008.
- [26] Y. Oktem, D. L. Balabanski, B. Akkus, C. W. Beausang, M. Bostan, R. B. Cakirli, R. F. Casten, M. Danchev, M. Djongolov, M. N. Erduran, S. Erturk, K. A. Gladniski, G. Gürdal, J. Tm. Goon, D. J. Hartley, A. A. Hecht, R. Krücken, N. Nikolov, J. R. Novak, G. Rainovski *et al.*, *Phys. Rev. C* **76**, 044315 (2007).
- [27] C. Y. Niu, A. C. Dai, C. Xu, H. Hua, S. Q. Zhang, S. Y. Wang, R. A. Bark, J. Meng, C. G. Wang, X. G. Wu, X. Q. Li, Z. H. Li, S. M. Wyngaardt, H. L. Zang, Z. Q. Chen, H. Y. Wu, F. R. Xu, Y. L. Ye, D. X. Jiang, R. Han *et al.*, *Phys. Rev. C* **97**, 034322 (2018).
- [28] K. Kimura, N. Takagi, and M. Tanaka, *Nucl. Phys. A* **336**, 246 (1980).
- [29] J. F. Lemming, J. Rapaport, and A. J. Elwyn, *Nucl. Phys. A* **239**, 412 (1975).
- [30] F. Hoyle *et al.*, *Nucl. Phys. A* **519**, 189 (1990).
- [31] E.-W. Grewe, C. Bäumer, H. Dohmann, D. Frekers, M. N. Harakeh, S. Hollstein, H. Johansson, L. Popescu, S. Rakers, D. Savran, H. Simon, J. H. Thies, A. M. van den Berg, H. J. Wörche, and A. Zilges, *Phys. Rev. C* **78**, 044301 (2008).
- [32] J. H. Thies, D. Frekers, T. Adachi, M. Dozono, H. Ejiri, H. Fujita, Y. Fujita, M. Fujiwara, E.-W. Grewe, K. Hatanaka, P. Heinrichs, D. Ishikawa, N. T. Khai, A. Lennarz, H. Matsubara, H. Okamura, Y. Y. Oo, P. Puppe, T. Ruhe, K. Suda *et al.*, *Phys. Rev. C* **86**, 014304 (2012).
- [33] D. Frekers, M. Alanssari, H. Ejiri, M. Holl, A. Poves, and J. Suhonen, *Phys. Rev. C* **95**, 034619 (2017).
- [34] D. Zinatulina, V. Brudanin, V. Egorov, C. Petitjean, M. Shirchenko, J. Suhonen, and I. Yutlandov, *Phys. Rev. C* **99**, 024327 (2019).
- [35] R. A. Haring-Kaye, R. M. Elder, J. Döring, S. L. Tabor, A. Volya, P. R. P. Allegro, P. C. Bender, N. H. Medina, S. I. Morrow, J. R. B. Oliviera, and V. Tripathi, *Phys. Rev. C* **92**, 044325 (2015).
- [36] J. Döring, D. Pantelică, A. Petrovici, B. R. S. Babu, J. H. Hamilton, J. Kormicki, Q. H. Lu, A. V. Ramayya, O. J. Tekyi-Mensah, and S. L. Tabor, *Phys. Rev. C* **57**, 97 (1998).

- [37] A. K. Mondal, A. Chakraborty, K. Mandal, U. S. Ghosh, A. Dey, S. Biswas, B. Mukherjee, and S. Rai, *Phys. Rev. C* **102**, 064311 (2020).
- [38] K. Starosta, T. Koike, C. J. Chiara, D. B. Fossan, D. R. LaFosse, A. A. Hecht, C. W. Beausang, M. A. Caprio, J. R. Cooper, R. Krücken, J. R. Novak, N. V. Zamfir, K. E. Zyromski, D. J. Hartley, D. L. Balabanski, J.-Y. Zhang, S. Frauendorf, and V. I. Dimitrov, *Phys. Rev. Lett.* **86**, 971 (2001).
- [39] T. Koike, K. Starosta, C. Vaman, T. Ahn, D. B. Fossan, R. M. Clark, M. Cromaz, I. Y. Lee, and A. O. Macchiavelli, in *Frontiers of Nuclear Structure*, FNS2002, Berkeley, CA, 2002, edited by P. Fallon and R. Clark, AIP Conf. Proc. No. 656 (AIP, New York, 2003), p. 160.
- [40] T. Koike, K. Starosta, and I. Hamamoto, *Phys. Rev. Lett.* **93**, 172502 (2004).
- [41] S. Y. Wang, S. Q. Zhang, Q. Bin, and J. Meng, *Chin. Phys. Lett.* **24**, 536 (2007).
- [42] S. Y. Wang, S. Q. Zhang, B. Qi, and J. Meng, *Phys. Rev. C* **75**, 024309 (2007).
- [43] S. Q. Zhang, B. Qi, S. Y. Wang, and J. Meng, *Phys. Rev. C* **75**, 044307 (2007).
- [44] S. Y. Wang, S. Q. Zhang, B. Qi, J. Peng, J. M. Yao, and J. Meng, *Phys. Rev. C* **77**, 034314 (2008).
- [45] S. Y. Wang, B. Qi, and D. P. Sun, *Phys. Rev. C* **82**, 027303 (2010).
- [46] C. Liu, S. Y. Wang, B. Qi, and Hui Jia, *Chin. Phys. Lett.* **37**, 112101 (2020).
- [47] P. A. Butler and W. Nazarewicz, *Rev. Mod. Phys.* **68**, 349 (1996).
- [48] A. Mukherjee, S. Bhattacharya, T. Trivedi, R. P. Singh, S. Muralithar, D. Negi, R. Palit, S. Nag, S. Rajbanshi, M. Kumar Raju, S. Kumar, D. Choudhury, R. Kumar, R. K. Bhowmik, S. C. Pancholi, and A. K. Jain, *Phys. Rev. C* **105**, 014322 (2022).
- [49] P. D. Cottle, J. W. Holcomb, T. D. Johnson, K. A. Stuckey, S. L. Tabor, P. C. Womble, S. G. Buccino, and F. E. Durham, *Phys. Rev. C* **42**, 1254 (1990).
- [50] K. Mandal, A. Chakraborty, A. K. Mondal, U. S. Ghosh, A. Dey, S. Biswas, B. Mukherjee, S. Rai, S. Chatterjee, S. K. Das, S. Samanta, R. Raut, S. S. Ghugre, S. Bhattacharyya, S. Nandi, S. Bhattacharya, G. Mukherjee, S. Ali, A. Goswami, S. Mukhopadhyay *et al.*, *Phys. Rev. C* **105**, 034328 (2022).
- [51] S. Rajbanshi, R. Palit, R. Raut, Y. Y. Wang, Z. X. Ren, J. Meng, Q. B. Chen, Sajad Ali, H. Pai, F. S. Babra, R. Banik, S. Bhattacharya, S. Bhattacharyya, P. Dey, S. Malik, G. Mukherjee, Md. S. R. Laskar, S. Nandi, Rajkumar Santra, T. Trivedi *et al.*, *Phys. Rev. C* **104**, 064316 (2021).
- [52] X. C. Han, C. Liu, and S. Y. Wang, *Int. J. Mod. Phys. E* **32**, 2340003 (2023).
- [53] M. Spieker, L. A. Riley, P. D. Cottle, K. W. Kemper, D. Bazin, S. Biswas, P. J. Farris, A. Gade, T. Ginter, S. Giraud, J. Li, S. Noji, J. Pereira, M. Smith, D. Weisshaar, and R. G. T. Zegers, *Phys. Rev. C* **106**, 054305 (2022).